FAR-IR AND SUBMILLIMETER RADIATION FROM COMETARY AND CIRCUMSTELLAR DUST

DAVID C. JEWITT

Institute for Astronomy, University of Hawaii, 2680 Woodlawn Drive,
Honolulu, HI. 96822.

ABSTRACT

Cometary and circumstellar dust grains may share a common origin in the accretion disks of pre main-sequence stars. Far-IR and submillimeter radiation from these grains may be used to infer basic characteristics of the dust. We discuss recent long wavelength measurements of comets and circumstellar dust clouds, and describe the problems inherent in their interpretation.

Keywords: Radio astronomy, dust, comets, young stars, planet formation

1. INTRODUCTION

This review was prepared from notes used in a "tutorial lecture" given at the 24th ESLAB Symposium held in Friedrichshafen, Germany, September 1990. Some of the informal style of that lecture has been retained in this written review, in the hope that the resulting text will be both readable and fully accessible to newcomers to this newest of research areas. The present article is intended as a deliberately simplified introduction to the emergent fields of cometary and stellar submillimeter astronomy, but it should not be regarded as a replacement for the original papers on which it is based. Because of space limitations, only a subset of the pertinent references can be listed, but I regard the subset as "core reading material" for this subject.

We define far-IR radiation as having wavelengths $20 \leq \lambda \leq 100$ μm and submillimeter radiation as having $0.1 \leq \lambda \leq 2$ mm. The definitions are arbitrary, of course, but reflect common usage. The main advantages of the far-IR and submillimeter regions of the electromagnetic spectrum to the observational astronomer are

(i). To probe cold dust, which does not emit strongly at conventional thermal infrared wavelengths because of the steepness of the short-wavelength side of the Planck function. For instance, the peak of the blackbody emission at temperature T = 10 K is at wavelength $\lambda \sim 300$ μm, at the short end of the submillimeter spectral range.

(ii). Submillimeter emission is sometimes in the Rayleigh-Jeans portion of the blackbody spectrum, in which the emission is a particularly simple function of the dust temperature. Thus uncertainties in the temperature of the emitting dust have a smaller effect on the interpretation of the emission than at shorter wavelengths near the blackbody maximum.

(iii). Far-IR and, especially, submillimeter dust grain opacities are small, so that many dust systems which are optically thick at short wavelengths are optically thin in the far-IR and submillimeter. This in turn allows the determination of total dust mass from the submillimeter flux.

The remainder of this review consists of 3 parts. First we will review pertinent optics of dust grains. Second, we will describe recent measurements and interpretations of submillimeter radiation from comets, and, third, from circumstellar dust.

2. GRAIN-OPTICS DEFINITIONS

As a result of diffraction, grains may absorb and scatter radiation with effective cross sections different from their geometrical cross sections (Ref. 1 and 2). It is usual to define scattering and emission "efficiencies" by

$$Q_s = \frac{\textit{scattering cross section}}{\pi a^2} \tag{1}$$

$$Q_a = \frac{\textit{absorption cross section}}{\pi a^2} \tag{2}$$

where a is the radius of an equal mass sphere. Since both scattering and absorption can remove radiation from a beam, the total extinction is the sum

$$Q_e = Q_a + Q_s. \tag{3}$$

We further define the albedo as the ratio of scattering to extinction for a particle, namely as

Proceedings of the 24th ESLAB Symp. on the Formation of Stars and Planets, and the Evolution of the Solar System, Friedrichshafen, 17-19 Sept. 1990 (ESA SP-315, Nov. 1990)

$$A = \frac{Q_s}{Q_e}. \qquad (4)$$

The Q's are functions of particle size, a, wavelength, λ, and of the wavelength-dependent complex refractive index $m(\lambda) = n(\lambda) - i\,k(\lambda)$. Since many optical effects depend on the ratio of particle size to wavelength, we finally define the dimensionless size parameter

$$x = \frac{2\pi a}{\lambda}. \qquad (5)$$

Measurements show that the Q's vary with x in a complicated way, shown schematically in Figure 1. Geometric optics ($Q_s = Q_a = 1$) may not be generally assumed.

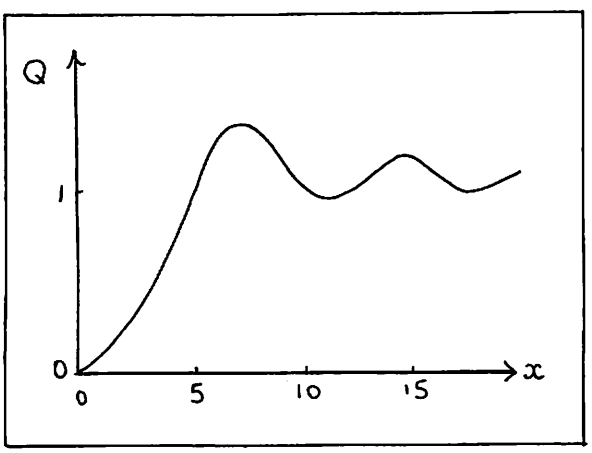

Figure 1. Schematic variation of Q_a with x for a spherical particle.

Note from the Figure that
(1). $Q_a \rightarrow 0$ as $x \rightarrow 0$.
(2). $Q_a \rightarrow$ constant as $x \rightarrow \infty$ (geometric optics limit).
(3). Q_a oscillates at intermediate x.
(4). Q_a has a maximum, which may be > 1, at $x \sim$ few.

$Q_a(a,\lambda,m)$ was first *calculated* by Mie in 1906 (see Ref. 1) - he solved Maxwell's equations using boundary conditions on the surface of a homogeneous sphere. While the Q's have been calculated for a few other geometries (notably, for infinitely long cylinders), their calculation for irregular and even (most) regular shapes is still a topic of frontier research.

Simple explanations of the ripples in Figure 1 have been offered, and are useful in understanding the underlying physics of Mie spheres. Consider two rays, one passing centrally through a spherical particle, the other grazing its surface, as shown in Figure 2.

The path length for ray 1 is $L_1 = 2a$ and that for ray 2, $L_2 = 2an$. The path length difference $\Delta L = 2a(n - 1)$ corresponds to $\Delta N = \Delta L / \lambda$ wavelengths, or, by eq. (5)

$$\Delta N = \frac{x(n - 1)}{\pi}. \qquad (6)$$

When combined (by the eye, or a lens), rays 1 and 2 will

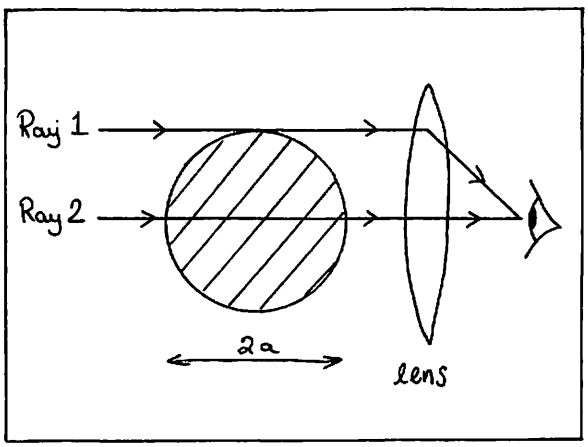

Figure 2. Origin of ripples in the Q's.

interfere constructively when $\Delta N = 1,2,3....$ giving

$$x_N = \frac{\pi N}{n - 1} \qquad (7)$$

for the location of the N'th interference maximum. A typical glass might have $n \sim 3/2$. By substitution, the first maximum of Q in a glass sphere would then occur at $x_1 \sim 2\pi \sim 6$, and subsequent maxima would have a characteristic spacing $\Delta x \sim 2\pi$ (c.f. Figure 1). The ripples seen in spheres of a single size (the uncomfortable term "monodisperse" is used to describe a set of particles of one size) are washed-out in naturally occurring size distributions, and are damped by asphericity, and by absorption in particles (obviously, ray 2 becomes progressively fainter as absorption increases). However, the first maximum at $a/\lambda \sim 1$ is a sufficiently gross feature as to survive. Its significance is that observations of particles in a size distribution are biassed towards particles with $a \sim \lambda$, since these are the most efficient radiators. Thus, we expect that submillimeter observations should be especially sensitive to the presence of submillimeter particles, whereas, for example, optical observations are biassed more towards particles with $a \sim 1\ \mu m$.

2.1 Rayleigh Regime

The limit $x \ll 1$ and $|mx| \ll 1$ is the Rayleigh regime. In this regime, the particle is small compared to the wavelength and all constituent oscillators experience the same electric field. The effect of the particle is then calculated as the sum of the fields of a set of in-phase dipoles, and gives particularly simple forms for Q_a and Q_s(Ref. 1). In this regime, for instance,

$$Q_a \propto x \propto \frac{a}{\lambda} \quad \text{and} \quad Q_s \propto x^4 \propto \left(\frac{a}{\lambda}\right)^4 \qquad (8)$$

giving the familiar Rayleigh scattering law and the somewhat less familiar Rayleigh absorption law. For small absorbing particles, the 4th power dependence on x guarantees that $Q_s \ll Q_a$, and in the submillimeter range, scattering is generally negligible compared to absorption and emission. Since $x \ll 1$ and so $Q_a \ll 1$ in the Rayleigh regime, it is often argued (or

assumed) that the submillimeter optical depth of astrophysical dust clouds is small (i.e. that the dust is optically thin in the submillimeter). When true, the submillimeter flux density radiated by a set of grains is just the sum of the emissions from the individual grains. We write

$$F_\nu \propto \sum_N Q_a \pi a^2 \qquad (9)$$

where the sum is taken over all N grains. With $Q_a \propto a/\lambda$, we see $F_\nu \propto \Sigma a^3$. But the total grain mass is $M \propto \Sigma a^3$, so that $F_\nu \propto M$. This is the origin of our previous statement that submillimeter photometry provides a (nearly) direct measure of the mass of emitting grains. The picture is not so simple if large grains ($x \geq 1$) exist, or if the optical depth is not small. We will see below that large grains in optically thick systems may be important in circumstellar clouds.

2.2 Uncertainties

Uncertainties in the Q's have two main origins.
(1). The compositions of the grains are uncertain. Since $Q_a = Q_a(a,\lambda,m)$ and $m = m(\lambda)$, the effective submillimeter Q_a's are uncertain, perhaps by an order of magnitude (see Figure 3).

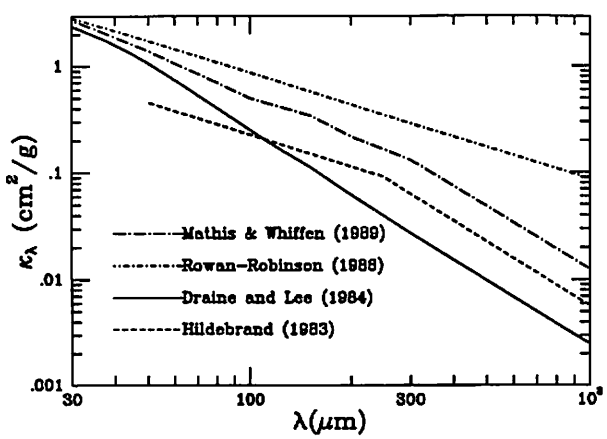

Figure 3. Various estimates of the submillimeter opacities of astrophysical dust (from Ref. 6).

(2). The shapes of the particles are uncertain. We are most comfortable with the optics of homogeneous spheres, but there are good reasons to suspect that grains in comets and circumstellar clouds may be highly non-spherical. These include
(i). Brownlee particles ($a \sim 10$ μm sized interplanetary grains collected from the stratosphere) display aggregate "bunch-of-grapes" structure.
(ii). Dense molecular clouds show anomalous extinction, suggesting agglomerative grain growth.
(iii). Particle sedimentation in circumstellar disks should promote additional rapid grain growth by aggregation, leading to open, possibly fractal, grain shapes (Ref. 3).

Therefore, we are interested to know Q_a for particles resembling that shown in Figure 4.

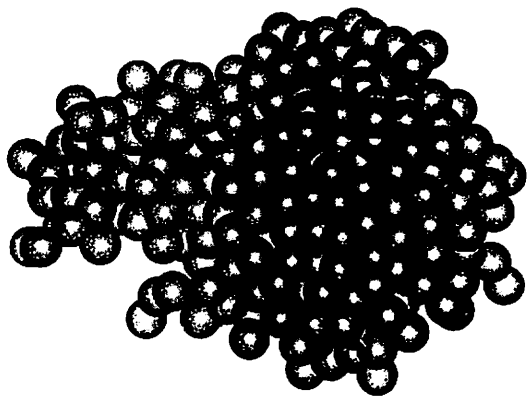

Figure 4. Aspherical particle produced by agglomeration of small spheres (Ref. 4).

A few specific cases have been studied (e.g. Ref. 3, 5). Typically, the opacities of open particles are at least an order of magnitude greater than those of equal mass spheres. Uncertainties in particle structure thus imply order of magnitude uncertainties in the effective opacity, and in derived particle masses (c.f. Ref. 6).

3. COMETS

For two reasons, the interpretation of submillimeter radiation from comets is much simpler than that from circumstellar dust. First, the comets are optically thin at all continuum wavelengths, so that radiative transfer in the cometary coma is trivial. Second, the geometry of the comet with respect to the heating source (the Sun) is well known, so that the dust temperature in a given comet can be calculated with some confidence. In the circumstellar dust, by contrast, there is no general guarantee that the system is optically thin (although this is likely to be true at submillimeter wavelengths except in the disk centers). Furthermore, the spatial distribution of the dust and the variation of its temperature with position are not known a-priori. For these reasons, it is convenient to examine long wavelength radiation in the simple cometary systems first, and then to expand the discussion to include the more complicated circumstellar systems.

Long wavelength emission from comets has been detected with confidence only in the past several years (Refs. 8, 9, 10). Most of the claimed detections are on the order of a few 10's to 100 mJy (1 mJy = 10^{-29} W m^{-2} Hz^{-1}) for comets at heliocentric distances $R \leq 1$ AU. For comparison, the weakest sources detectable at 0.8-mm with the James Clerk Maxwell Telescope have $F_\nu \sim 15$ - 20 mJy and require integrations of hours. The comets are thus painfully weak sources of long wavelength continuum radiation. Observations of P/Halley at 1.3-mm over 10 days in 1986 are shown in Figure 5. Within the uncertainties of measurement, the data are consistent with a constant 50 mJy source. The nucleus of P/Halley is

particularly well characterized, and is too small to account for the observed submillimeter emission - an origin in the coma is implied.

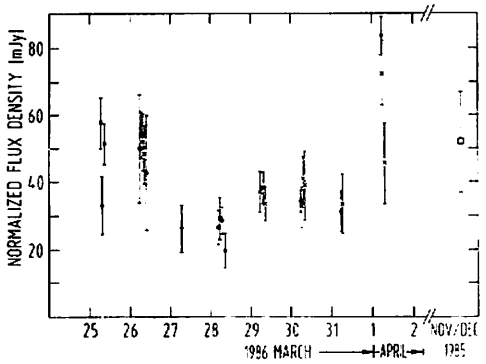

Figure 5. Submillimeter radiation from comet P/Halley (Ref. 8).

The first submillimeter spectrum of a comet is shown in Figure 6 (Ref. 9). The spectral index, α, ($F_\nu \propto \lambda^{-\alpha}$) is $\alpha \leq 3$.

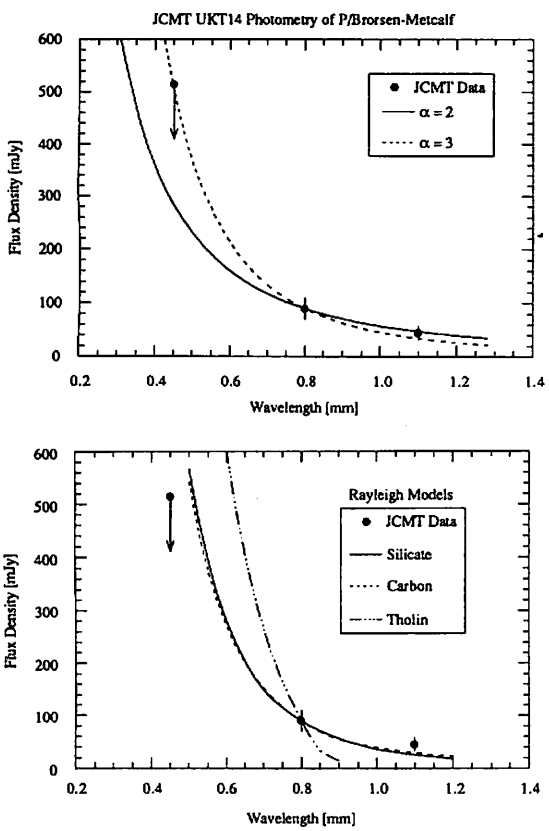

Figure 6. (a). Submillimeter spectrum of Comet Brorsen-Metcalf (Ref. 9). Lines show power law spectra with indices α = 2 and α = 3. (b). Rayleigh models for three grain compositions. The models are normalized to the datum at 0.8-mm. All Rayleigh models have spectral indices steeper than α = 3, and thus do not match the data.

The cometary emission from Comet Brorsen-Metcalf is presumably thermal radiation from dust, since there is insufficient plasma for free-free radiation to be detectable, and (again), the nucleus is too small to account for the measured flux density. A very simple model of the cometary emission is possible since

(i). The geometry of the source is perfectly known.
(ii). The coma is optically thin.
(iii). The dust temperature is easy to calculate.

We present the simple model as a counterpoint to the more involved (less certain) models of emission from circumstellar dust, in which the geometry is not well known, the system may be optically thick in parts, and the dust temperature varies spatially. We will show that considerable uncertainties exist even in the simple cometary case, and thus (by implication) that equal or larger uncertainties must exist in the interpretation of circumstellar emission.

The thermal flux density from an optically thin coma is (Ref. 9)

$$F_\nu = \int_{a-}^{a+} \frac{B_\nu(T(a))\, Q_a(a,\lambda,m)\, \pi a^2\, n(a)\, da}{\Delta^2} \qquad (10)$$

where $n(a)da$ is the differential size distribution taken as

$$n(a)\, da = \Gamma a^{-s}\, da \qquad (11)$$

and $3 \leq s \leq 4$ is suggested by Halley Giotto and Vega (Ref. 10) data. The minimum and maximum particle sizes are a- and a+, respectively. In the Rayleigh-Jeans limit ($h\nu/(kT) \ll 1$)

$$B_\nu(T(a)) \sim \frac{2\, k\, T(a)}{\lambda^2} \qquad (12)$$

and so

$$F_\nu = \frac{2\, \pi\, k\, \Gamma}{\lambda^2\, \Delta^2} \int_{a-}^{a+} T(a)\, Q_a(a,\lambda,m)\, a^{2-s}\, da. \qquad (13)$$

For a given composition and for spherical particles, $Q_a(a,\lambda,m)$ can be computed from Mie theory. The likely size distribution is constrained by spacecraft data, although the appropriate values of a- and a+ are uncertain. The grain temperature may be calculated from the equation of radiative balance

$$\int_0^\infty Q_a\, \pi a^2\, \frac{S_\nu^{sun}}{R^2}\, d\nu = \int_0^\infty 4\, \pi a^2\, Q_a\, \pi B_\nu(T(a))\, d\nu \qquad (14)$$

in which S_ν^{sun} is the solar flux density incident on a grain of radius a at heliocentric distance R. The integral on the left gives the total absorbed solar power, while that on the right gives the total emitted power, assuming that the grain is

isothermal (hence the factor 4). Since S_ν^{sun} peaks near $\lambda \sim 0.5$ μm while $B_\nu(T(a))$ peaks near $\lambda \sim 10$ μm , it is apparent that the grain temperature at a given R is controlled by $Q_a(0.5\mu m)/Q_a(10\mu m)$, and is thus material and size-dependent. Grains may be either hotter or cooler than blackbodies at the same R depending on whether $Q_a(0.5\mu m)/Q_a(10\mu m)$ is > 1 or < 1. Note that single photon heating (Ref 11) which influences the mean temperatures of interstellar grains, is negligible in the cometary case since the sun is a weak source of UV photons.

The mass of the grains responsible for the submillimeter radiation may be calculated from

$$M = \frac{4}{3}\pi\rho\Gamma\int_{a-}^{a+} a^{3-s}\,da \tag{15}$$

The constant Γ is determined for a given model by eq. (13).

The models computed from eq. (9) - (13) depend on a-, a+, s, and $m(\lambda)$, all of which are imperfectly known. The resultant models are thus non-unique, even in this ideally simple case. However, examination of a large number of models leads to two results of probable significance (Ref 11).
(i). The total grain mass in Brorsen-Metcalf is $M \sim 10^9$ - 10^{10} kg for all models employed. The implied dust production rates are $dM/dt \sim 10^4$ - 10^5 kg s^{-1}, comparable to the mass lost per second from P/Halley near perihelion.
(ii). The small submillimeter spectral index is incompatible with an origin in pure Rayleigh particles (for which $\alpha \sim 4$ is found, versus $\alpha \leq 3$ observed). Sample Rayleigh models are shown in Fig. 6b. The existence of optically large particles ($x \geq 1$, or $a \geq 1$mm) is implied.

These conclusions are valid within the spherical particle model of the emission. If the particles are instead porous agglomerates, the estimates of M will be too high. In addition, Wright (1987) remarks that fractal particles tend to produce relatively flat spectra, perhaps providing a second explanation for the small observed spectral index in Brorsen-Metcalf.

4. Circumstellar Dust

The photospheres of most stars are invisible at submillimeter wavelengths. For instance, the sun at 10pc would contribute only 0.3 mJy at $\lambda \sim 1$ mm, and could not be detected with present technology. Certain young stars, notably the T-Tauri stars, do exhibit clear submillimeter emission, however, and this emission is best ascribed to thermal radiation from circumstellar dust. Excess radiation in the thermal IR is also attributed to dust, although at shorter wavelengths photospheric emission constitutes a larger fraction of the flux (and at longer (e.g. cm) wavelengths, free-free radiation from plasma is proportionately more significant). A few main-sequence stars also exhibit non-photospheric submillimeter radiation (Ref. 12), including the famous cases α Lyr (Vega) and β Pic, revealed by IRAS.

What is the evidence that the circumstellar dust exists in *disks*, as opposed to some other geometrical configuration? There appear to be 4 circumstantial arguments for the existence of dust disks.

(i). The Extinction Argument
The quantity of circumstellar dust needed to supply the submillimeter emission is much larger than the amount inferred from measurements of visual extinction towards the T-Tauri stars. This very simple and powerful argument is often stated without elaboration in the literature. It seems worthwhile to examine it in more detail by means of a simple model in which dust occupies a spherically symmetric distribution about a star, with number density

$$N_1(r) = N_1(r_0)\left(\frac{r_0}{r}\right)^p \tag{16}$$

and in which the dust temperature is given by

$$T(r) = T(r_0)\left(\frac{r_0}{r}\right)^q. \tag{17}$$

Here, r_0 corresponds to the inner edge of the disk, and $r_0 \leq r \leq R$ is the radial distance from the star. As a further simplification, we assume that emission from the dust occurs entirely in the Rayleigh-Jeans limit (the essence of the argument is not changed by this assumption). The flux density from a spherical dust shell of thickness dr is then

$$dF_\nu = \left(4\pi r^2\,dr\,N_1(r)\right)\left(\frac{Q_a^{sm}\pi a^2}{\Delta^2}\right)\left(\frac{2kT(r)}{\lambda^2}\right) \tag{18}$$

where Q_a^{sm} denotes the grain absorption efficiency at submillimeter wavelengths (say, $\lambda \sim 1$ mm). In eq. (18), the first bracketed term is the number of particles in the shell, the second is the effective solid angle subtended by one particle at geocentric distance Δ, and the last bracketed term is the Planck function. Substitution of eq. (16) and (17) and integration with respect to radius gives

$$F_\nu = \left(\frac{8\pi k Q_a^{sm}\pi a^2 N_1(r_0)\,r_0^{p+q}\,T_0}{\lambda^2\Delta^2}\right)\left[\frac{r^{3-p-q}}{3-p-q}\right]_{r_0}^{R} \tag{19}$$

provided $p+q \neq 3$ (the case $p+q = 3$ is equally trivial - we omit it here to save space).

The visual optical depth along a line of sight to the star is

$$\tau_\nu = \int_{r_0}^{R} N_1(r)\,Q_e^\nu\,\pi a^2\,dr \tag{20}$$

where Q_e^ν denotes the extinction efficiency in the visual. Using eq. (16), eq. (20) becomes

$$\tau_\nu = N_1(r_0)\,r_0^p\,Q_e^\nu\,\pi a^2\left[\frac{r^{1-p}}{1-p}\right]_{r_0}^{R} \tag{21}$$

provided $p \neq 1$. The ratio of visual optical depth to submillimeter flux density is

$$\frac{\tau_\nu}{F_\nu} = \left(\frac{Q_e^\nu}{Q_a^{sm}}\right)\left(\frac{\lambda^2 \Delta^2}{8\,\pi\, k\, T(r_0)\, r_0^q}\right)\left(\frac{3 - p - q}{1 - p}\right)\frac{\left[r^{1-p}\right]_{r_0}^{R}}{\left[r^{3-p-q}\right]_{r_0}^{R}}. \qquad (22)$$

For example, with r_0 = 1 AU, R = 100 AU, $T(r_0)$ = 100 K, q = 0.5, p = 1.4, Δ = 100 pc (all suggested by observations and theoretical considerations), eq. (22) gives

$$\frac{\tau_\nu}{F_\nu[Jy]} \sim 6\left(\frac{Q_a^\nu}{Q_e^{sm}}\right) \qquad (23)$$

where F_ν is now expressed in Janskys. For low albedo particles we may write $Q_e^\nu \sim Q_a^\nu$. Then $\tau_\nu/F_\nu \sim 6\, Q_a^\nu/Q_a^{sm}$, and the ratio of the Q_a's can be obtained from Mie theory or from other studies. For instance,

$Q_a^\nu/Q_a^{sm} \sim few \times 10^2$ for porous grains, while

$Q_a^\nu/Q_a^{sm} \sim few \times 10^3$ for Mie spheres.

Therefore, we find

$$\tau_\nu \sim (600 - 6000)\, F_\nu\,[Jy] \qquad (24)$$

for the particular example considered here. A 1 Jy source would exhibit $\tau_\nu \sim 600 - 6000$ if the dust were arranged about the star in spherical symmetry. This is huge compared to the typical visual extinction towards T-Tauri stars, $\tau_\nu \sim 1$, from which it is inferred that the dust cannot be spherically distributed about the star. Distributions which place the bulk of the dust out of the line of sight to the central star are needed to simultaneously satisfy the submillimeter and visual extinction data. This does not point exclusively towards a disk geometry, but it is consistent with a disk geometry.

(ii). Asymmetries of Emission Lines

The T-Tauri stars eject winds, which emit in various optical forbidden lines. Examined at high spectral resolution, the line profiles are generally seen to be asymmetric, with a strong blue wing and a weak or absent red wing (Ref. 13). Since the T-Tauri stars cannot preferentially eject matter towards earth, it is suggested that the red wing due to receding wind is preferentially extinguished by a dust disk in the vicinity of the star. Again, this inference does not point unambiguously to a disk, since any dust distribution around the star will tend to obscure the more distant receding matter relative to the near-side blue-shifted matter.

(iii). High Resolution Imaging

A few T-Tauri stars show evidence of asymmetric extended emission, which may indicate the presence of disks. Unfortunately, the nearest star forming regions (in Taurus, Ophiuchus) are at distance $\Delta \sim 150$ pc, so that 1" ~ 150 AU. Disks of 100 AU radial extent thus subtend angles ~ 1", and are very difficult to study from the ground (or from the defective Space Telescope, for that matter).

(iv). Polarization Maps

A few near infrared polarization maps show spatial asymmetries consistent with scattering in flattened dust structures.

While not individually compelling, the four arguments taken together carry considerable weight, and suggest that the circumstellar dust is distributed in disks around T-Tauri stars.

How can we model the submillimeter emission from a dust disk? Allowing for a finite optical depth, we may write

$$F_\nu = \frac{\cos\theta}{\Delta^2}\int_{r_0}^{R} B_\nu(T(r))\,[1 - exp(-\tau_\nu)]\,2\,\pi\, r\, dr \qquad (25)$$

where θ is the angle of inclination of the disk to the line of sight, the disk extends from r_0 to R, and the other symbols are as previously defined (c.f. Refs. 15, 16, 17). The optical depth through the disk is

$$\tau_\nu = \frac{\kappa_\nu\, \Sigma(r)}{\cos\theta} \qquad (26)$$

in which κ_ν [m^2 kg^{-1}] is the grain opacity at frequency ν, and $\Sigma(r)$ [kg m^{-2}] is the disk mass surface density. For a single sphere, the opacity is related to Q_a by $\kappa_\nu = 3\, Q_a/(4\, \rho\, a)$. Although it is tempting to assume that the disks are optically *thin* in the submillimeter (after all, that is why the submillimeter is so useful for the determination of disk properties!), the more massive disks are optically *thick* in their centers even at mm wavelengths. The form of $\Sigma(r)$ depends on complex physical processes inside the disk, and is not known. In the presence of planet formation, $\Sigma(r)$ may not even be a monotonic function of r. For convenience a power-law form is adopted for the surface density

$$\Sigma(r) = \Sigma(r_0)\left(\frac{r_0}{r}\right)^p \qquad (27)$$

Similarly, the radial variation of the temperature is determined by the detailed energy balance of the disk, and is poorly understood. The energy source of the disk is some combination of stellar radiation absorbed and then re-emitted by the disk, plus internal luminosity due to frictional heating and energy liberated by infalling matter. A perfectly flat, optically thick, infinite disk would intercept exactly $L_*/4$, where L_* is the stellar luminosity (Ref. 17). There are good physical reasons to expect that disks are flared (thickness increases with radius), in which case a larger fraction of the stellar luminosity can be absorbed and the radial temperature gradient is decreased. Only in very high luminosity systems, $L \geq L_*$, can we be sure that intrinsic disk luminosity is important. To hide our ignorance of the true temperature structure, it is convenient to parameterize the temperature with a power law (c.f. eq. 17).

The variables in this most simple disk model include

q	inclination
$T(r_0)$, q	temperature structure
κ_ν	opacity (size distribution, composition)
$\Sigma(r_0)$, p	surface density structure
r_0, R	disk dimensions.

It is remarkable that a model with so many free parameters can be constrained by far-IR and submillimeter data. However, a number of approximations are possible. For instance, in the limit $\tau_\nu \rightarrow \infty$ (corresponding to the shorter infrared wavelengths, or to a disk seen edge-on), 1- $\exp(-\tau_\nu) \rightarrow 1$, and eq. (25) can be shown to yield $F_\nu \propto \nu^{(3 - 2/q)}$. Therefore, a determination of the spectral index in the optically thick limit leads directly to the temperature index, q. Values found by Beckwith *et al.* (1990) cluster in the range $q \sim 0.5$ - 0.7.

The temperature index is (weakly) diagnostic of the physical process responsible for disk heating. For instance, in an optically thin disk the absorbed stellar power varies as r^{-2} while the radiated power from a blackbody varies as T^4, so that $T \propto r^{-0.5}$, i.e. $q = 1/2$. In a disk which is optically thick at visual wavelengths, the index is $q = 3/4$, essentially because the r^{-2} variation of the stellar flux is reduced further by a projection factor which varies as R_*/r, where R_* is the stellar radius, so that $T^4 \propto r^{-3}$. Coincidentally, the temperature dependence expected in a massive disk heated by internal viscous dissipation is also $q = 3/4$ (Ref. 18). In other words, the diagnostic power of q is limited, but it is at least interesting that empirical values of q fall in the 1/2 - 3/4 range expected from simple considerations.

In the optically thin case, $\tau_\nu \ll 1$, 1- $\exp(-\tau_\nu) \rightarrow \tau_\nu$, and the emitted spectrum is independent of θ, but proportional to κ_ν so reviving all of the problems encountered already in modelling the cometary emission (Ref. 19). The more massive disks will tend to be optically thick in the submillimeter at small r and thin towards the outer edge, so that the interpretation is more complicated than suggested by either of the two limiting cases discussed. The reader is directed to Ref. 16 for practical examples of model fitting.

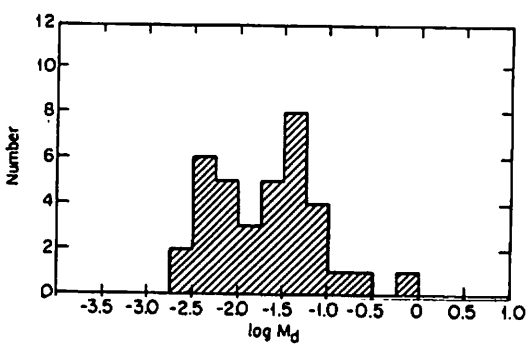

Figure 7. Histogram of disk masses for T-Tauri stars determined from submillimeter data by Beckwith et al. (Ref. 16). The disk masses have been scaled from measured dust masses by a factor ~100, to account for the gas/dust mass ratio.

One parameter of great interest is the total mass of dust (Figure 7). Figure 7 shows that the disk masses inferred from submillimeter data are in the range $10^{-2.5}$ to 1 M_{sun}. The present mass of the planets and comets is of order 10^{-3} M_{sun}. The so-called minimum-mass solar nebula (determined by augmenting the present solar system to cosmic composition) had $M_{mmsn} \sim 10^{-2}$ M_{sun}. Evidently, the T-Tauri disks are comparable to M_{mmsn} allowing the possibility of planet formation. Indeed, some of the disks appear to have masses comparable to their central stars, in which case rapid planet formation by spontaneous gravitational collapse might be unavoidable. As previously noted, the empirical masses are uncertain by at least one order of magnitude, but even if the masses plotted in Fig. 7 are uniformly reduced by a factor of 10, a great many T-Tauri disks contain enough mass to produce planetary systems like our own.

The disks are destroyed by viscous dissipation, causing material to fall onto the central star and to recede to large distances, or by planet formation. A constraint on the timescale for disk dissipation is suggested by Figure 8.

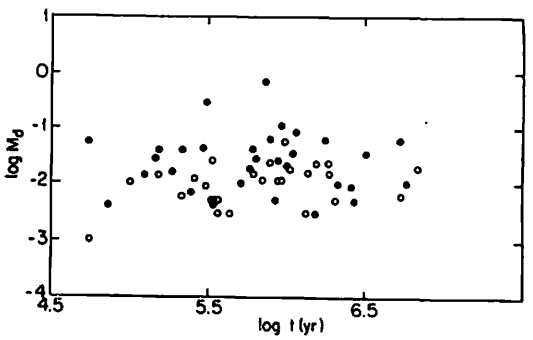

Figure 8. Inferred disk mass versus the age of the underlying T-Tauri star, again from Ref. 16.

Evidently, the disk mass shows no trend with stellar age up to ~10^7 years, suggesting that mass is not substantially depleted on shorter timescales. The absence of points at ages > 10^7 years in Fig. 8 signifies the difficulty of identifying pre-main-sequence stars in the post T-Tauri phase, and does not imply that older disks are absent. Similar considerations based on 10 μm IR data suggest disk depletion on timescales ~ 3 x 10^6 - 10^7 years (Ref. 20). The IR and submillimeter timescales can be reconciled if the disks are depleted first at their inner edge (where the high temperatures produce the bulk of the 10 μm signal), leaving cooler outer material to provide the submillimeter emission.

One more puzzle concerns the relation of the dust around pre-main-sequence stars to the dust in T-Tauri systems. The main-sequence-stars have dust masses of order 10^{-8} M_{sun}(Ref. 12), corresponding to total masses (dust + gas) of order 10^{-6} M_{sun}. Thus, they are weaker than the T-Tauri systems by 3 - 6 orders of magnitude. The main-sequence stars are about 10^9 years old. One possibility is that the main-sequence emission is from the last remnants of a formerly massive disk, the bulk of the

material having been collected into planets. A second possibility is that the main-sequence emission is from dust released from orbiting parent-bodies in recent times. The Sun is surrounded by a dust cloud (the "Zodiacal Cloud") replenished on 10^5 year timescales by comets, although the mass of this cloud is only $\sim 10^{-15} M_{sun}$. To properly understand the evolution of disks we need a measurement of the disk mass as a function of stellar age for stars intermediate in age between the T-Tauri stars and the main sequence stars into which they evolve.

5. REFERENCES

1. van de Hulst, H. C. (1957). Light Scattering by Small Particles, John Wiley & Sons, New York.
2. Bohren, C. F., and Huffman, D. R. (1983). Absorption and Scattering of Light by Small Particles, John Wiley & Sons, New York.
3. Wright, E. L. (1987). Long Wavelength Absorption by Fractal Dust Grains. Ap. J., 320, 818.
4. Jewitt, D., and Meech, K. (1988). Optical Properties of Cometary Nuclei and a Preliminary Comparison With Asteroids. Ap. J., 328, 974.
5. Hage, J. I., and Greenberg, J. M. (1990). A Model for the Optical Properties of Porous Grains. Ap. J., 361, 251.
6. Draine, B. T. (1990). Mass Determinations from Far-Infrared Observations, to appear in The Interstellar Medium in Galaxies, edited by H. A. Thronson and J. M. Shull, Dordrecht, Kluwer.
7. Altenhoff, W. J., Huchtmeier, W. K., Schmidt, J., Schraml, J. B., Stumpff, P., and Thum, C. (1986). Astron. Astrophys., 164, 227.
8. Altenhoff, W. J., Huchtmeier, W. K., Kreysa, E., Schmidt, J., Schraml, J. B., and Thum, C. (1989). Astron. Astrophys., 222, 323.
9. Jewitt, D., and Luu, J. (1990). The Submillimeter Continuum of Comet P/Brorsen-Metcalf, Ap. J., in press (December 20 issue).
10. McDonnell, J. A. M. *et al.* (1987). Dust Distribution Within The Inner Coma Of Comet P/Halley: Encounter By Giotto's Impact Detectors. Astron. Ap., 187, 719.
11. Sellgren, K. (1984). The Near-IR Continuum Emission of Visual Reflection Nebulae. Ap. J., 277, 623.
12. Becklin, E. E., and Zuckerman, B. (1989). Submillimeter Emission from Small Dust Grains Orbiting Nearby Stars, Kona Submillimeter Conference preprint.
13. Cabrit, S., Edwards, S., Strom, S. E., and Strom, K. M. (1990). Forbidden Line Emission and Infrared Excesses in T-Tauri Stars: Evidence for Accretion-Driven Mass Loss. Ap. J., 354, 687.
14. Adams, F. C., Lada, C., and Shu, F. H. (1987). Spectral Evolution of Young Stellar Objects. Ap. J., 312, 788.
15. Adams, F. C., Emerson, J. P., and Fuller, G. A. (1990). Submillimeter Photometry and Disk Masses of T-Tauri Disk Systems. Ap. J., 357, 606.
16. Beckwith, S. V. W., Sargent, A. J., Chini, R. S., and Güsten, R. (1990). A Survey for Circumstellar Disks Around Young Stellar Objects. A. J., 99, 924-944.
17. Hildebrand, R. H. (1983). The Determination of Cloud Masses and Dust Characteristics from Submillimetre Thermal Emission. Q. Jl. R. astr. Soc., 24, 267-282.
18. Lynden-Bell, D., and Pringle, J. (1974). The Evolution of Viscous Disks and the Origin of the Nebular Variables. M. N. R. A. S., 168, 603.
19. Weintraub, D. A., Sandell, G., and Duncan, W. D. (1989). Submillimeter Measurements of T Tauri and FU Orionis Stars. Ap. J., 340, L69-L72.
20. Skrutskie, M. F., Dutkevitch, D., Strom, S. E., Edwards, S., and Strom, K. M. (1990). A Sensitive 10 μm Search for Emission Arising from Circumstellar Dust Associated with Solar-Type Pre-Main Sequence Stars. A. J., 99, 1187.